



## An optical study of self-assembled In x Ga 1-x As/GaAs quantum dots embedded in a two-dimensional electron gas

E. Ribeiro, F. Cerdeira, M. J. S. P. Brasil, T. Heinzl, K. Ensslin, G. Medeiros-Ribeiro, and P. M. Petroff

Citation: *Journal of Applied Physics* **87**, 7994 (2000); doi: 10.1063/1.373485

View online: <http://dx.doi.org/10.1063/1.373485>

View Table of Contents: <http://scitation.aip.org/content/aip/journal/jap/87/11?ver=pdfcov>

Published by the [AIP Publishing](http://www.aip.org)

---

### Articles you may be interested in

[Optical properties of low-strained In x Ga 1 - x As/Ga As quantum dot structures at the two-dimensional–three-dimensional growth transition](#)

*J. Appl. Phys.* **100**, 013503 (2006); 10.1063/1.2208296

[Studies of band alignment and two-dimensional electron gas in In Ga P N/Ga As heterostructures](#)

*Appl. Phys. Lett.* **86**, 061103 (2005); 10.1063/1.1855406

[Effects of two-dimensional electron gas on the optical properties of InAs/GaAs quantum dots in modulation-doped heterostructures](#)

*Appl. Phys. Lett.* **86**, 021916 (2005); 10.1063/1.1849853

[A photomodulated reflectance study of InAs/GaAs self-assembled quantum dots](#)

*Appl. Phys. Lett.* **73**, 3268 (1998); 10.1063/1.122740

[Transport properties of two-dimensional electron gases containing InAs self-assembled dots](#)

*Appl. Phys. Lett.* **73**, 2468 (1998); 10.1063/1.122484

---

**Not all AFMs are created equal**  
**Asylum Research Cypher™ AFMs**  
**There's no other AFM like Cypher**

[www.AsylumResearch.com/NoOtherAFMLikeIt](http://www.AsylumResearch.com/NoOtherAFMLikeIt)

  
OXFORD  
INSTRUMENTS  
The Business of Science®

The advertisement features a dark blue background with a film strip graphic on the left. The text is in white and orange. The Oxford Instruments logo is in the bottom right corner.

# An optical study of self-assembled $\text{In}_x\text{Ga}_{1-x}\text{As}/\text{GaAs}$ quantum dots embedded in a two-dimensional electron gas

E. Ribeiro,<sup>a)</sup> F. Cerdeira, and M. J. S. P. Brasil

*Instituto de Física "Gleb Wataghin," Universidade Estadual de Campinas, Caixa Postal 6165, 13083-970 Campinas-SP, Brazil*

T. Heinzel and K. Ensslin

*Laboratorium für Festkörperphysik, ETH Zürich, CH8093 Zürich, Switzerland*

G. Medeiros-Ribeiro<sup>b)</sup> and P. M. Petroff

*Materials Department, University of California, Santa Barbara, California 93106*

(Received 22 October 1999; accepted for publication 15 February 2000)

We studied the low temperature (77 K) photomodulated reflection and transmission as well as the photoluminescence at 2.2 K of a self-assembled  $\text{In}_x\text{Ga}_{1-x}\text{As}$  quantum dot layer grown on a (100) GaAs substrate in the vicinity of a two-dimensional electron gas. The dot layer was grown without rotation of the substrate in order to achieve a gradual variation of the In concentration along the wafer diameter. This resulted in an increase in the density of quantum dots along the In concentration gradient, which is reflected in a characteristic dependence of the relative intensities of the spectral lines. A consistent assignment of the optical structure observed in all spectra leads to an estimate of the average value of the Fermi energy in the conduction band of the wetting layer ( $E_F \approx 13.4$  meV). The variation of this Fermi energy along the composition gradient can be obtained from the spectra, and an estimate of the gradient of the density of quantum dots along this direction can be made. A careful comparison of the variation of the critical energy of the different lines suggests that the average quantum dot size depends on the In molar fraction of the alloy, which is seen to vary more or less linearly across the wafer diameter. © 2000 American Institute of Physics. [S0021-8979(00)06510-5]

## I. INTRODUCTION

The importance of zero-dimensional systems, both for basic physics and for device applications,<sup>1</sup> has motivated developments in epitaxial growth that led to the controlled growth mode of self-assembled quantum dots (SAQDs). With this method, a layer of a lattice-mismatched material (e.g., InAs) grows commensurate to the substrate (GaAs) until a critical thickness is reached when islanding starts spontaneously on top of the two-dimensional (2D) wetting layer, giving rise to high-quality, defect-free quantum dots with good size uniformity.<sup>2-4</sup> These self-assembled quantum dots are randomly distributed in the plane and have been extensively studied by optical techniques, such as photoluminescence (PL).<sup>5-8</sup> The information obtained by PL, however, is restricted to the lower-energy states. Although far-infrared spectroscopy<sup>9,10</sup> and PL excitation<sup>11</sup> also give information about higher-energy states, modulation spectroscopy techniques are particularly suitable for broad characterization of semiconductor heterostructures.<sup>12</sup> This alternative tool has been recently used to study large SAQDs and the wetting layer (WL) on top of which the dots grow.<sup>13-15</sup> The presence of a two-dimensional electron gas (2DEG) gives rise to special physical properties. Electrical measurements have shown that small ( $\sim 200$  Å diam) InAs SAQDs can tailor the trans-

port properties (e.g., the mobility) of an AlGaAs/GaAs 2DEG as the number of SAQDs per unit area (dot density) varies.<sup>16</sup> For the highest QD densities, SAQDs have also driven a surprising metal-insulator transition for electrons in GaAs,<sup>17</sup> a phenomenon still not understood which requires detailed characterization of SAQDs embedded in a 2DEG.

Recently, Ribeiro *et al.* reported the growth of an InAs SAQD layer without rotation of the GaAs substrate in order to achieve a gradual variation of the In concentration along the wafer diameter.<sup>16</sup> This resulted in an increase in the density of quantum dots along the In flux gradient, and no significant change in the average size of the dots. Here we report the growth of an  $\text{In}_x\text{Ga}_{1-x}\text{As}$  SAQD layer by the same means, i.e., without rotation of the substrate. The average In concentration corresponds to an incorporated average molar fraction  $\bar{x} = 0.24$  in the alloy. For this case, we have an additional degree of freedom which is the alloy composition of the mismatched layer. Therefore, in contrast to Ref. 16, the flux gradient here will be reflected in a molar fraction gradient of the alloy layer and this, in turn, might result in a variation of the average size of the quantum dots as well as the expected variation in their spatial density. In order to characterize in detail the SAQDs produced by this procedure, we studied the low-temperature photomodulated reflection (PR), transmission (PT), and photoluminescence spectra of a series of samples of identical dimensions, cut from a region near the center of the wafer, following the In flux gradient.

<sup>a)</sup>Electronic mail: evaldo@ifi.unicamp.br

<sup>b)</sup>Present address: Laboratório Nacional de Luz Síncrotron, Caixa Postal 6192, 13083-970 Campinas-SP, Brazil.

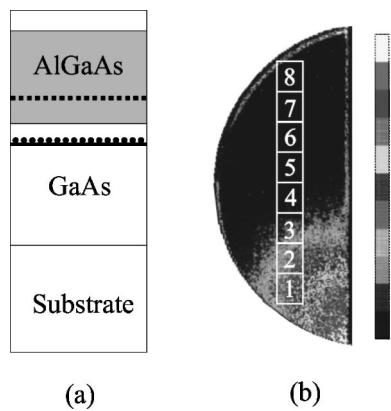


FIG. 1. (a) Sketch of the structure used in the present study. (b) PL map of the wafer (see Ref. 16). The In coverage decreases from top to bottom.

We were able to identify electronic transitions that originate in the quantum dots as well as others that involve wetting layer states. From the evolution of these transitions with sample number, we infer the changes in QD density, alloy composition, and size along the In flux gradient.

## II. EXPERIMENTAL DETAILS

The heterostructure used in this work was grown by molecular beam epitaxy (MBE) on a GaAs (001) substrate. Figure 1(a) shows a sketch of the wafer. After growth of a buffer layer of GaAs and an  $\text{In}_x\text{Ga}_{1-x}\text{As}$  WL (nominally  $x=0.24$ ) of 58 monolayers, a plane of SAQDs formed and was immediately covered by 30 Å of GaAs and 1400 Å of  $\text{Al}_{0.3}\text{Ga}_{0.7}\text{As}$  and capped with 100 Å of GaAs. The carriers for the 2DEG are provided by Si  $\delta$  doping within the barrier 300 Å towards the sample surface from the AlGaAs/GaAs heterointerface. The SAQD layer was grown without rotation of the substrate, so that the In flux impinging on the structure varied gradually along the wafer diameter. This gradient of In coverage should produce a gradient in the dot density. Transmission electron microscopy (TEM) and transport experiments in a wafer of InAs SAQDs grown under similar conditions have identified such a gradient of the dot density with a constant average dot size throughout the wafer.<sup>16</sup> As in Ref. 16, a photoluminescence map is able to identify the gradient of the dot density in our wafer [see Fig. 1(b)]. Furthermore, since the SAQDs and the WL material are an alloy ( $\text{In}_x\text{Ga}_{1-x}\text{As}$ ), the gradient of the In flux might also lead to an additional gradient in the In molar fraction  $x$ . Samples  $S_1$ – $S_8$  were cleaved and numbered following the gradient line, shown in Fig. 1(b), so that the In flux increases for an increasing sample number.

Photomodulated reflectance and transmission spectra were taken at 77 K using a standard setup.<sup>12</sup> Modulation is achieved by a chopped (200 Hz) He–Ne laser and the probe beam is the light of a tungsten lamp dispersed by a 1 m Spex spectrometer. The light reflected (transmitted) is detected by a Si photodiode and fed into a PAR124A lock-in amplifier. PL measurements were performed at 2 K. A 5145 Å line of an Ar laser ( $\sim 120 \text{ W/cm}^2$ ) was used for excitation and the emission was analyzed by a 0.5 m Spex monochromator and detected by a photomultiplier.

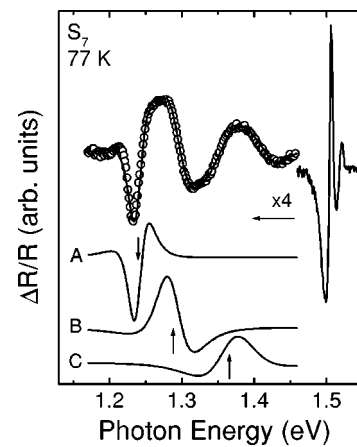


FIG. 2. PR spectrum of sample  $S_7$ , showing the GaAs fundamental gap ( $\approx 1.5 \text{ eV}$ ) and the structures that originated in the  $\text{In}_x\text{Ga}_{1-x}\text{As}$  layer (lower energies). This last portion of the spectrum (open dots) is fitted (continuous trace) with lines A, B, and C, shown independently below for the sake of clarity.

## III. RESULTS

The photomodulated reflectance spectrum of sample  $S_7$  is shown in Fig. 2. The strongest structures in the spectrum correspond to the fundamental transition in GaAs and their associated Franz–Keldysh oscillations.<sup>12,13</sup> At lower photon energies a number of weaker features appear which we attribute to transitions within the  $\text{In}_x\text{Ga}_{1-x}\text{As}$  SAQD layer. These transitions were fitted with standard modulated reflectivity line shapes, as described in Ref. 13. This fitting procedure is illustrated in the main body of Fig. 2, where open dots represent experimental data while the solid curve is the result of the fit. Below this curve, the individual line shapes used for each transition are shown, with arrows indicating the optical transition energy associated with each of these curves. Three transitions, labeled A, B, and C, respectively, are clearly identified in all our spectra in order of increasing photon energy. An additional weak structure, D, (not shown) is also present in all spectra, close to the GaAs band gap ( $\sim 1.43 \text{ eV}$ ), and might be associated with a shallow impurity on GaAs.<sup>18</sup> We follow this fitting procedure for all samples. Representative spectra of samples  $S_2$ ,  $S_4$ , and  $S_7$ , in the relevant photon energy range, are shown in Fig. 3. Figure 4 displays the dependence of the transition energies obtained from the PR and PT spectra versus the sample number,  $n$ . Their linear decrease with increasing  $n$  suggests that the In molar fraction of the alloy in these samples  $S_n$  increases linearly with  $n$ . The slopes of these lines, obtained from linear regression, are listed in Table I. Also listed in Table I are the transition energy and the linewidth for each line, averaged over all samples. Before discussing the significance of these results, we will describe the photoluminescence experiments.

Representative PL spectra are displayed in Fig. 5, and show two different lines, labeled  $\alpha$  and  $\beta$ , respectively, in order of increasing photon energy. Line  $\alpha$  has a significantly larger linewidth compared to line  $\beta$  (see Table I). Both lines have peak positions which decrease linearly with the sample number (see the inset in Fig. 5), but the slope of the transi-

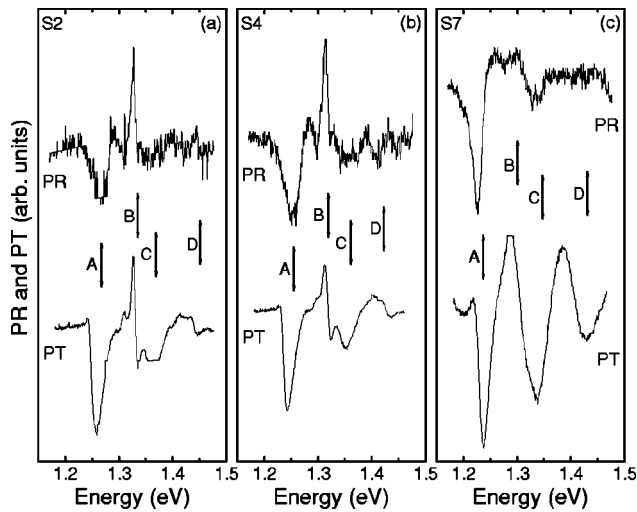


FIG. 3. PR and PT spectra of samples (a)  $S_2$ , (b)  $S_4$ , and (c)  $S_7$ , in the photon energy range below the GaAs band gap. Arrows indicate the energy positions of the four structures present in all spectra of the series of samples.

tion energies of  $\alpha$  is steeper, by a factor of about 3, than that of transition  $\beta$  (see Table I).

#### IV. DISCUSSION

In a multicomponent sample, where light traverses many layers of different compositions and/or morphology, it is not always easy to identify the part of the sample responsible for a given spectral feature. In our samples, the absolute energy minima for electrons and holes occur within the  $\text{In}_x\text{Ga}_{1-x}\text{As}$  alloy. Hence, we expect that electron-hole recombinations take place within the portion of the sample containing this alloy. The PL lines are interpreted in terms of recombinations from the conduction band of the wetting layer and/or QDs to the topmost unoccupied state created in the valence band of these structures by the exciting radiation. Notice that the transition energies listed in Table I for either modulated reflectivity or PL peaks lie below the gap of GaAs (AlGaAs) but above the gap of the bulk  $\text{In}_x\text{Ga}_{1-x}\text{As}$  alloy with a nominal composition  $\bar{x}=0.24$ , even when the effects of strain are

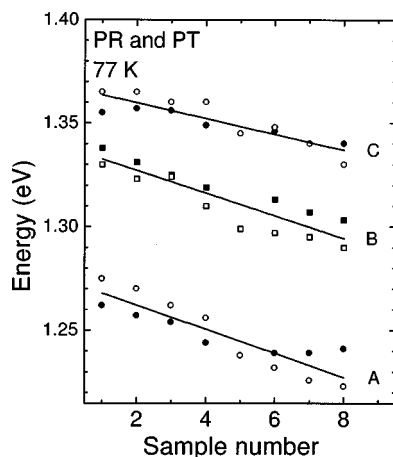


FIG. 4. Energy position of lines A, B, and C plotted as a function of sample number (In content). Open (closed) symbols represent data from PR (PT) spectra. The lines are linear fits to the data.

TABLE I. Slopes of the linear dependence of the transition energies vs  $n$  obtained from PL, PR, and PT spectra; average values, over all the samples, of the transition energies and linewidths [full width at half maximum (FWHM)]; assignments of the observed transitions (see Fig. 6). Labeling of the different lines follows the convention used in Figs. 3 and 5 (LH=light hole).

Technique	Line	$(\Delta E/\Delta n)$ (meV)	$\bar{E}_j$ (eV)	FWHM (meV)	Assignment
PL	$\alpha$	$18 \pm 2$	1.223	36	$\text{QD}_e \rightarrow \text{QD}_h$
PL	$\beta$	$5.5 \pm 0.3$	1.246	4	$\text{WL}_e(0) \rightarrow \text{QD}_h$
PR+PT	A	$5.8 \pm 0.8$	1.250	36	$\text{QD}_h \rightarrow \text{WL}_e(E_F)$
PR+PT	B	$5.5 \pm 0.7$	1.315	19	$\text{WL}_h \rightarrow \text{WL}_e(E_F)$
PR+PT	C	$3.8 \pm 0.5$	1.348	50	$\text{LH} \rightarrow \text{WL}_e(E_F)(?)$

taken into account.<sup>18–20</sup> This is compatible with our interpretation in terms of optical transitions within the mismatched layer. This assignment is reinforced in the case of modulation spectroscopy (lines A, B, and C), since they appear both in the reflectivity and transmission spectra, and the other portions of the sample are too thick to give a significant contribution to the latter.

We now try to assign the five spectral lines listed in Table I to electronic transitions between states of the QDs or WL. Our assignments are based on a calculation of the electronic structure by Hawrylak and Wojs<sup>21</sup> for systems similar to ours. Although quantitative comparison is not possible, the general ordering of the electronic energy levels calculated by these authors can be adapted to identify the structure observed in our spectra. Our assignments are summarized in the last column of Table I and illustrated in Fig. 6. QD (WL) designate states confined within the quantum dots (wetting layer) and the subindex  $e(h)$  indicate an electron (heavy hole) state. Because of the presence of a 2DEG [see Fig. 1(a)], we expect the electron states in the QDs to be fully occupied and those in the WL to be occupied up to the Fermi energy ( $E_F$ ) within its two-dimensional continuum. Hence, all absorption (reflection) lines have final states above the  $\text{WL}(E_F)$ , while the final state in recombination corresponds

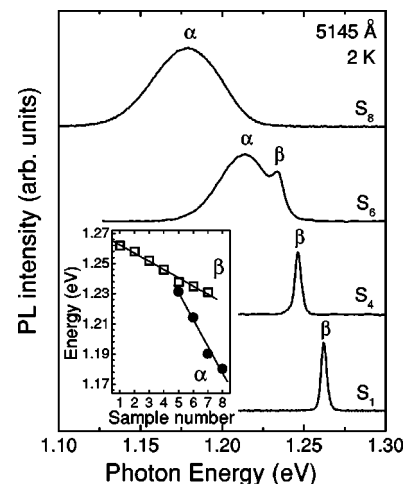


FIG. 5. PL spectra of samples  $S_1$ ,  $S_4$ ,  $S_6$ , and  $S_8$  showing the evolution of lines  $\alpha$  and  $\beta$ . The inset presents the energy positions of lines  $\alpha$  and  $\beta$  vs sample number  $n$ .

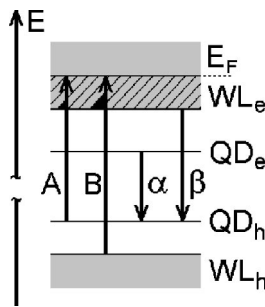


FIG. 6. Sketch of the valence and conduction bands used for identifying experimental lines A, B,  $\alpha$ , and  $\beta$ . The conduction band of the wetting layer is filled with electrons up to the Fermi energy  $E_F$ .

to the highest valence band state in the WL+QD system, i.e.,  $QD_h$ . Initial states for recombination are expected to be the lowest occupied states in either the quantum dot or the bottom of the conduction band of the wetting layer, i.e.,  $QD_e$  or  $WL(0)$ . This logic is reflected in the assignments in Table I, the justification of which is discussed below.

In relation to the lines in the modulation spectroscopy spectra, two facts are easily discernible (see Figs. 2 and 3 and the numerical data listed in Table I): (i) line B is much narrower than lines A or C; (ii) the intensity of lines A and C relative to that of line B increases monotonically with increasing sample number  $n$ . These facts are consistent with attributing line B to transitions between states which involve exclusively the wetting layer, since this layer should remain uniform and constant in width throughout the wafer.<sup>2-4,16</sup> In contrast, the QDs have a size distribution, which translates itself into a spread of the valence band levels and an even greater spread (smaller effective mass) of the conduction band levels. This makes the transitions beginning or ending in QD states broader than those which involve only states of the WL. Also, the density of SAQDs should increase with increasing  $n$ ,<sup>16</sup> in line with the increase in the intensity of the spectral lines involving quantum dot states. These considerations give a solid basis for identifying lines A and B as  $QD_h \rightarrow WL(E_F)$  and  $WL_h \rightarrow WL(E_F)$ , respectively. The assignment of line C is more uncertain. We believe that it probably involves a transition from a light hole state to WL ( $E_F$ ). The light hole in 2D systems of similar materials is practically unconfined.<sup>18</sup> It is not clear, however, how the complex WL+SAQD system affects this state. Both the line-width of line C and the evolution of its relative intensity with  $n$  point to a transition starting in a state sensitive to QD size and density. Hence, the assignment of this line to a light hole to conduction band transition depends on the ability of the QD to confine this type of hole. Since this assignment is only tentative, we have placed a question mark next to it in Table I. The assignment of emission lines  $\alpha$  and  $\beta$  to  $QD_e \rightarrow QD_h$  and  $WL_e(0) \rightarrow QD_h$ , respectively, is straightforward given the considerations discussed above. This identification is reinforced by the fact that the first line is much broader than the second (greater sensitivity of the conduction band QD states to the size distribution) and that line  $\alpha$  is stronger in samples with a larger number of QDs (larger  $n$ ).<sup>22</sup>

The self-consistency of the assignments made above is brought into focus when examining the actual transition energies and their linear dependence on the sample number (the slopes of the straight lines  $E_j$  vs  $n$  of Figs. 4 and 5, listed in Table I). First, we notice that the relationship between the transition energies of lines A in the PR or PT spectra and  $\beta$  in the PL ought to be given by

$$E(A) + \Delta = E(\beta) + E_F, \quad (1)$$

where  $\Delta$  is, roughly, the temperature increase in the gap of the bulk  $In_xGa_{1-x}As$  alloy of average composition from 77 to 2 K,<sup>13</sup> and  $E_F$  is the Fermi energy in the 2D conduction band of the wetting layer. Using the transition energies in Table I,  $\Delta \approx 8$  meV (see Refs. 13 and 23) yields a value of  $E_F \approx 12$  meV for the average Fermi energy. From this value we calculate an average carrier density of  $N_s \approx 3.2 \times 10^{11} \text{ cm}^{-2}$ , which is in agreement with the level of doping in the sample.<sup>16</sup> Moreover, the slope of the line  $E(A)$  vs  $n$  is slightly, albeit consistently, steeper than that of the  $E(\beta)$  vs  $n$  line (Table I). This trend [Eq. (1)] indicates that the Fermi energy suffers a slight decline with increasing  $n$ . This is a natural consequence of the increase in the number of SAQDs: as we increase  $n$ , more electrons will fall into QD states, which will partially deplete the conduction band of the wetting layer. The slopes listed in Table I predict a decrease of 14% in  $E_F$  ( $12.6 \text{ meV} \leq E_F \leq 14.3 \text{ meV}$ ) from samples  $S_1-S_8$ , with consequent variation in the carrier density in the wetting layer of  $3.0 \times 10^{11} \text{ cm}^{-2} \leq N_s \leq 3.4 \times 10^{11} \text{ cm}^{-2}$ . Assuming two electrons per dot,<sup>16,21</sup> this implies an increase in the QD density by a factor of approximately  $2 \times 10^{10} \text{ QD/cm}^2$  from samples  $S_1-S_8$ , consistent with the results of Ref. 16. The slope of  $E(B)$  vs  $n$  should directly reflect the variation in molar fraction  $x$  of the  $In_xGa_{1-x}As$  alloy as a function of the sample number, since the width of the wetting layer is assumed to be constant throughout and the weak variation in Fermi energy with  $n$  can be ignored here. Since the variation of the alloy gap with In composition, around an average molar fraction of  $\bar{x} \approx 0.24$ , is well known,<sup>18</sup> the slope of  $E(B)$  vs  $n$  can be used directly to estimate the change in In molar fraction in the wetting layers of our samples. This simple calculation yields a linear variation from  $x \approx 0.22$  to  $\approx 0.25$  from samples  $S_1-S_8$ . The similarity between the slopes of lines A, B, and  $\beta$  indicates that variation of the indium molar fraction in the alloy is basically the main factor responsible for the slopes in the straight lines of their transition energies versus  $n$ . Since the first and the last of these lines involve a transition to or from the  $QD_h$  state, we infer that the In molar fraction in the WL and QDs of each sample are probably the same, i.e., no In segregation occurs that dramatically changes the composition of the QDs in relation to that of the wetting layer.

The last conclusion depends on the assumption that the confinement energy of the heavy hole is not strongly dependent upon the changes in barrier height implied by the small variations in molar fraction discussed here.<sup>24</sup> While this is not easy to test, we tried to gain some insight into this issue by calculating such changes for a 2D quantum well with alloy compositions between  $x = 0.21$  and 0.26 and widths between 20 and 30 Å. Very little dependence for the confine-

ment energy with  $x$  was found in these cases for the heavy hole and a larger (but still small) dependence was found for the electron states. On the other hand, for a fixed composition, the heavy hole confinement energy changed very little with quantum well width while the confinement energy of the electronic state changed sharply. Hence, the assumptions made about the heavy hole state being relatively insensitive to small changes in In molar fraction and/or dimensions of the QDs seem justified. On the other hand, electronic QD states should be very sensitive to changes in size of the QDs but not as much to changes in the depth of the confining potential. With these results in mind, we compare the slope of  $E(\alpha)$  vs  $n$  and those of the other lines. Let us focus on the slopes of the transition energies of lines  $\alpha$  and  $\beta$ . The first is a factor of 3 larger than the second. Since the steeper line involves the  $QD_e$  state and the other does not, we must conclude, in view of the above discussion, that the average size of the quantum dots increases with increasing In molar fraction (increasing sample number). Based on a simple 2D calculation, this change in average size is *very roughly* estimated as 10% from  $S_1$ – $S_8$ . This simply means that the average quantum dot size increases as the In molar fraction does, which is not unreasonable to assume.

## V. SUMMARY AND CONCLUSIONS

We presented an optical study of a self-assembled  $\text{In}_x\text{Ga}_{1-x}\text{As}$  quantum dot layer grown on a (100) GaAs substrate in the vicinity of a two-dimensional electron gas. The  $\text{In}_x\text{Ga}_{1-x}\text{As}$  layer, which includes the dots plus a wetting layer, was grown without rotation of the substrate in order to achieve a gradual variation of the In flux along a wafer diameter. This resulted in an increase of the spatial density of quantum dots along the In gradient axis. We studied the low temperature (77 K) photomodulated reflectivity and transmission as well as the 2 K photoluminescence of a series of samples cleaved sequentially along the gradient line. The progressive variation in dot density is reflected in a characteristic dependence of the relative intensities of the spectral lines: for increasing In flux, structures related to the quantum dots present a continuous increase in their intensities relative to those that originate in the 2D wetting layer. The observation of a progressive energy shift of the spectral features along the gradient of the In flux also indicates the presence of a gradient of the In molar fraction  $x$  of the alloy. A consistent assignment of the optical structures observed in all spectra leads to an estimate of the Fermi energy in the conduction band of the wetting layer for each sample. From the changes in the Fermi energy we estimated the quantum dot density variation along the In gradient line. In addition, the magnitude of the energy shifts for each optical transition of the spectra across the gradient indicates that the average

quantum dot volume increases with increasing In molar fraction of the alloy.

## ACKNOWLEDGMENTS

The authors gratefully acknowledge financial support from Fundação de Amparo à Pesquisa do Estado de São Paulo, Conselho Nacional de Desenvolvimento Científico e Tecnológico, Schweizerische Nationalfonds, and QUEST.

- <sup>1</sup>H. Sakaki, Surf. Sci. **267**, 623 (1992).
- <sup>2</sup>D. Leonard, M. Krishnamurthy, C. M. Reaves, S. P. Denbaars, and P. M. Petroff, Appl. Phys. Lett. **63**, 3203 (1993).
- <sup>3</sup>J. M. Moison, F. Houzay, F. Barthe, L. Leprince, E. André, and O. Vatel, Appl. Phys. Lett. **64**, 196 (1994).
- <sup>4</sup>D. Leonard, K. Pond, and P. M. Petroff, Phys. Rev. B **50**, 11687 (1994).
- <sup>5</sup>S. Fafard, D. Leonard, J. L. Merz, and P. M. Petroff, Appl. Phys. Lett. **65**, 1388 (1994).
- <sup>6</sup>J.-Y. Marzin, J.-M. Gérard, A. Izraël, D. Barrier, and G. Bastard, Phys. Rev. Lett. **73**, 716 (1994).
- <sup>7</sup>R. Leon, P. M. Petroff, D. Leonard, and S. Fafard, Science **267**, 1966 (1995).
- <sup>8</sup>F. Adler, M. Geiger, A. Bauknecht, D. Haase, P. Ernst, A. Dornen, F. Scholz, and H. Schweizer, J. Appl. Phys. **83**, 1631 (1998).
- <sup>9</sup>H. Drexler, D. Leonard, W. Hansen, J. P. Kotthaus, and P. M. Petroff, Phys. Rev. Lett. **73**, 2252 (1994).
- <sup>10</sup>M. Fricke, A. Lorke, J. P. Kotthaus, G. Medeiros-Ribeiro, and P. M. Petroff, Europhys. Lett. **36**, 197 (1996).
- <sup>11</sup>R. Heitz *et al.*, Appl. Phys. Lett. **68**, 361 (1996).
- <sup>12</sup>F. H. Pollak, Superlattices Microstruct. **10**, 333 (1991); F. Cerdeira, Braz. J. Phys. **23**, 1 (1993).
- <sup>13</sup>L. Aïgouy, T. Holden, F. H. Pollak, N. N. Ledentsov, V. M. Ustinov, P. S. Kop'ev, and D. Bimberg, Appl. Phys. Lett. **70**, 3329 (1997).
- <sup>14</sup>G. L. Rowland, T. J. C. Hosea, S. Malik, D. Childs, and R. Murray, Appl. Phys. Lett. **73**, 3268 (1998).
- <sup>15</sup>G. Şek, J. Misiewicz, K. Ryczko, M. Kubisa, F. Heinrichsdorff, O. Stier, and D. Bimberg, Solid State Commun. **110**, 657 (1999).
- <sup>16</sup>E. Ribeiro, E. Müller, T. Heinzel, H. Auderset, K. Ensslin, G. Medeiros-Ribeiro, and P. M. Petroff, Phys. Rev. B **58**, 1506 (1998).
- <sup>17</sup>E. Ribeiro, R. D. Jäggi, T. Heinzel, K. Ensslin, G. Medeiros-Ribeiro, and P. M. Petroff, Phys. Rev. Lett. **82**, 996 (1999).
- <sup>18</sup>C. Vázquez-López, E. Ribeiro, F. Cerdeira, P. Motisuke, M. A. Sacilotti, and A. P. Roth, J. Appl. Phys. **69**, 7836 (1991).
- <sup>19</sup>G. Ji, D. Huang, U. K. Reddy, T. S. Henderson, R. Houdré, and H. Morkoç, J. Appl. Phys. **62**, 3366 (1987).
- <sup>20</sup>Y. Zou, P. Grodzinski, E. P. Menu, W. G. Jeong, P. D. Dapkus, J. J. Alwan, and J. J. Coleman, Appl. Phys. Lett. **58**, 601 (1991).
- <sup>21</sup>P. Hawrylak and A. Wojs, Semicond. Sci. Technol. **11**, 1516 (1996).
- <sup>22</sup>Notice that it is not easy to compare the full width at half maximum (FWHM) of PL and PR (or PT) spectra. First, both types of experiments were performed at different temperatures. More importantly, the FWHMs are related to the lifetime broadening of the intervening states through assumptions about the model line shapes. Thus, the numerical values of the numbers listed in Table I are strongly dependent upon the line shapes chosen. This should not affect the arguments comparing lines A, B, and C (or  $\alpha$  and  $\beta$ ) among one another. The same comparison is not easy for the FWHMs of these two sets (A with  $\alpha$  or B with  $\beta$ , for example).
- <sup>23</sup>Landolt-Börnstein New Series, edited by O. Madelung (Springer, Berlin, 1982), Vol. III/17a.
- <sup>24</sup>Average barrier heights are 173 meV for electrons and 98 meV for heavy holes. The molar fraction variation of  $\Delta x/x = 12.5\%$  would produce a corresponding variation in these barrier heights.